

# Topographical Structure of Solid Films of Poly[5,7-dodecadiyne-1,12-diols(4-butoxycarbonyl methylurethane)] Self-Assembled from Its Lyotropic Liquid Crystal Phase<sup>†</sup>

Kee Chua Toh and Wei Wang\*

Institute of Materials Research and Engineering, 3 Research Link, National University of Singapore, Singapore 117602

Received September 21, 1999; Revised Manuscript Received December 30, 1999

**ABSTRACT:** The topographical structures of film samples of a soluble polydiacetylene—poly[5,7-dodecadiyne-1,12-diols(4-butoxycarbonylmethylurethane)]—solidified from its lyotropic liquid crystal phase were characterized by means of scanning electron microscopy and atomic force microscopy. The observations reveal a structural feature of extended-chain lamellae of the film samples and furthermore a three-dimensional chain segregation with respect to molecular length in a layer thinner than 5 nm on the free surface of the samples.

## Introduction

It is well-known that soluble rigid shape persistent macromolecules usually exhibit a wormlike chain conformation in solution, so they will self-assemble into an ordered state, namely, a lyotropic liquid crystal phase when the polymer concentration gradually raises to a critical concentration.<sup>1,2</sup> The liquid crystal feature enables us to expect that structures and properties of the polymers in solid state will be highly dependent on structures and properties formed in their liquid crystal phase. At the early stage of studying liquid crystal behaviors of rigid macromolecules, it was assumed that the liquid crystal phase formed possesses a *nematic* feature simply due to a consideration of the most important feature of polymers: molecular length distribution.<sup>2</sup> In liquid crystal physics, the term of *nematics* describes a liquid crystal state of rigid molecules that has no long-range order but contains some orientational order: all molecules tend to be parallel to some common axis microscopically, and they will smoothly change their directors macroscopically.<sup>3</sup> Therefore, such the nematic feature seems to further imply that there is no special supermolecular structure able to form in the liquid crystal phase of rigid macromolecule solutions.

In 1977 de Gennes noted that splay deformation become difficult in a nematic composed of rigid macromolecules because of a limited number of chain ends.<sup>4</sup> This difficulty is reflected by very large splay constants increasing with molecular length. In 1981, Meyer furthered this basic idea and expected that rigid macromolecules would tend to self-assemble into extended-chain lamellae in their “nematic” phase to achieve a minimal density fluctuation caused by splay.<sup>5</sup> These theoretical studies were carried out without considering molecular length distribution. Such extended-chain lamellae have been confirmed by some experimental observations of the thin film samples solidified from the lyotropic phase of a soluble polydiacetylene {poly[5,7-dodecadiyne-1,12-diols(4-butoxycarbonylmethylurethane)] (P-4BCMU)} by means of transmission electron

microscopy (TEM).<sup>6–12</sup> It is very important to emphasize here that the extended-chain lamellae were observed in this polydiacetylene with a number-average molecular weight  $\bar{M}_n = 2.16 \times 10^5$  and a polydispersity index  $\bar{M}_w/\bar{M}_n = 2.14$ . The lamellae observed have different thicknesses and tapered shapes, originally relating to molecular length distribution. This finding shows for the first time the formation of the extended-chain lamellar structure through two-dimensional (2D) chain segregation with respect to chain length distribution. The chain segregation is associated with the longitudinal and transversal migrations of rigid macromolecules occurring in the “nematic” state.<sup>12</sup> On the basis of these results, we see that supermolecular structures formed by rigid macromolecules are very different from those obtained in conventional flexible chain polymers. In this work, we would like to report some new observations on extended-chain lamellae formed in the casting film samples of P-4BCMU by using either scanning electron microscopy (SEM) or atomic force microscopy (AFM). Because these techniques provide topographical structure information on sample surfaces, our observations will further demonstrate a three-dimensional (3D) chain segregation.

## Experimental Section

The polymer used is a soluble polydiacetylene (P-4BCMU), which is the same as the polymer used in the previous works.<sup>6–12</sup> It has a number-average molecular weight of  $\bar{M}_n = 2.16 \times 10^5$  and a polydispersity index  $\bar{M}_w/\bar{M}_n = 2.14$ .<sup>10</sup> Because the molecular weight of its repeating unit is 508, the number-average degree of polymerization,  $\bar{DP}$ , is about 425. Correspondingly, the average molecular length is about 205 nm since the length of the repeating unit is 0.48 nm.

The film samples with a thickness of about 500 nm were prepared by casting a couple of drops of the dilute solution (2 g/L) of the polymer in chloroform onto the surface of a cover glass, and then the glass was immediately moved into a weight glass plugged by a glass cover. The polymer concentration of the solution drop would increase because of evaporation of chloroform in solution until the equilibrium of chloroform vapor in the weight glass was reached. The film specimens on the cover glass surface had one free surface. The solid samples for further investigation were prepared by slowly solidifying the specimens in the weight glass.

\* To whom correspondence should be addressed.

<sup>†</sup> On the occasion of the 60th birthday of Prof. Dr. Gerhard Wegner

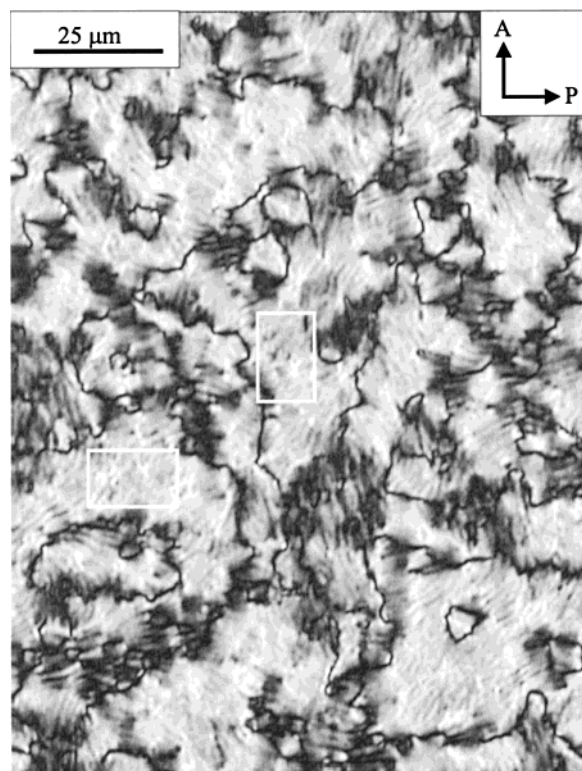


**Figure 1.** PLM image of this polydiacetylene showing a typical Schlieren texture of nematics.

The optical texture of P-4BCMU film samples in lyotropic phase and also in the solid state were studied by polarized light microscopy (PLM) (Nikon Optiphot2-Pol). Further, a field-emission scanning electron microscopy (FE-SEM) (Philips XL30) equipped with a secondary electron detector was utilized to characterize topographical morphology of the free surface of the solidified samples. Before carrying on SEM measurements, the free surface of the samples was coated with a thin gold layer with a thickness about 30 Å to avoid a charging effect. Meanwhile, an atomic force microscopy (Digital Instruments DI-3000) with the controller IIIa were applied to record the surface profiles of the free surface of the solidified sample. To minimize the inelastic deformation of the sample, the tapping mode was employed in this work to attain the height, amplitude, and phase images. The characteristic size of structural features presented in this study was determined by using the 2D fast Fourier transform (FFT) operation of the image analysis program (NIH Image Analysis 1.62).

## Results and Discussion

At first it is necessary to emphasize that, under the condition used for the sample preparation, the solution in the weight glass was in the lyotropic liquid crystal phase, which had been confirmed by the observations with PLM, showing the typical optical texture of nematics.<sup>8</sup> In this experiment, no grease was used to perfectly seal the gap between the weight glass rim and the cover, in order to get a slow leakage of chloroform vapor. In so doing, the solution stayed in the lyotropic phase for a longer time so as to annihilate as many defects as possible; thus a sample with coarsened liquid crystal texture was prepared. At the same time, the structures already developed in the lyotropic phase at different length scales will not be blurred or destroyed by a slow evaporation of solvents. Figure 1 shows the optical texture observed in a solidified sample. It is the same as or at least very similar to the texture obtained in lyotropic phase. This indicates that the liquid crystal texture as well as the supramolecular structure self-

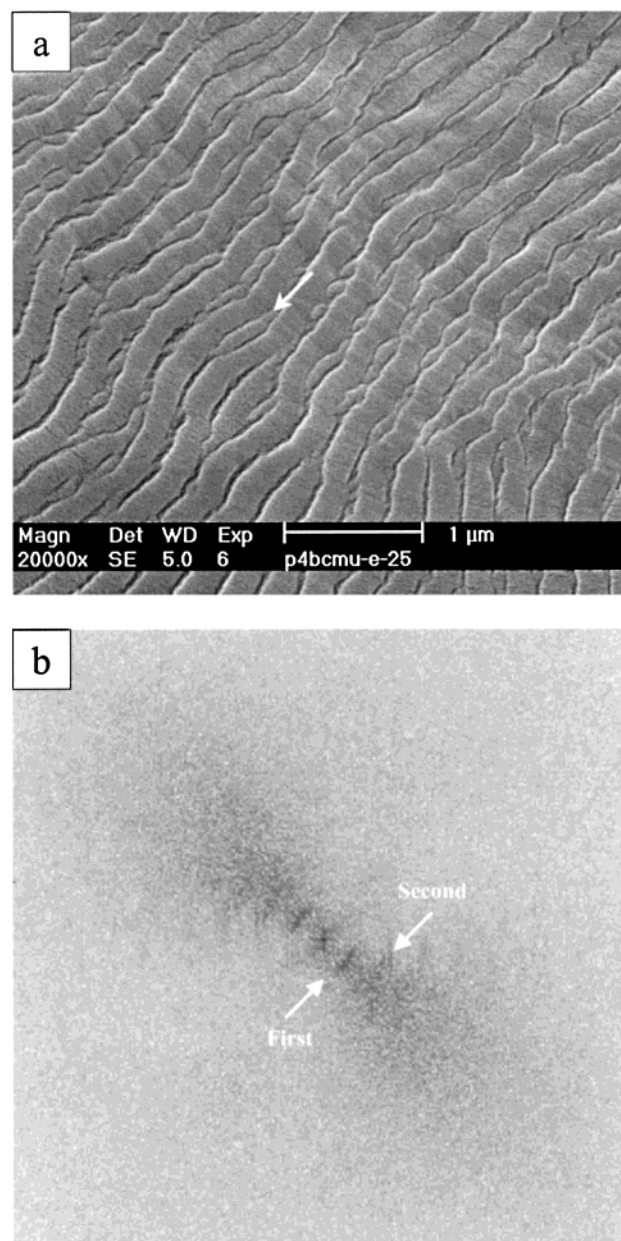


**Figure 2.** (a) SEM image showing the structural feature of extended-chain lamellae of the polymer. (b) Corresponding 2D FFT pattern.

assembled in lyotropic phase had been conserved in the solid samples to a great extent.<sup>8</sup> In the specimen, the average distance between adjacent defects is larger than many tens of micrometers. In accordance with the dividing of textural evolution given in ref 8, the sample used is in the late stages of defect annihilation. The following characterizations were performed in the area without defects. For example, the areas are enclosed by the square frames in Figure 1.

In contrast to the former works,<sup>6–12</sup> we are now more interested in topographical structures developed on the free surface of the film samples. Thus, SEM and AFM were employed to further characterize the solidified specimens because these techniques can provide information about the topography of a specimen surface. Figure 2a shows a typical structural feature of our specimens obtained by using SEM. Figure 2b shows the corresponding 2D FFT pattern. The SEM image exhibits a lamella-type morphological feature. In 2D FFT pattern at least first and second orders can be identified. These



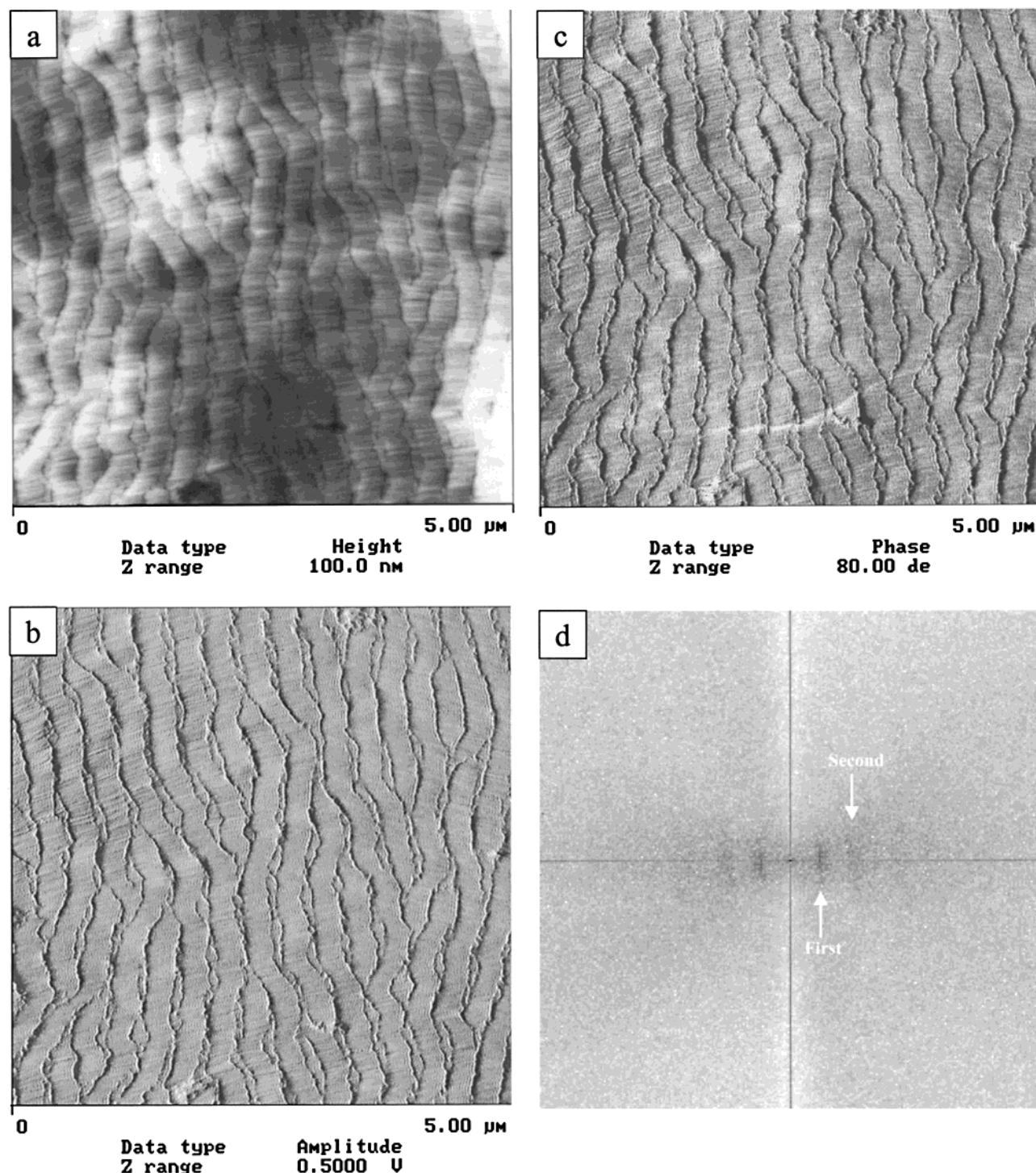


**Figure 3.** AFM height (a), amplitude (b), and phase (c) images showing the extended-chain lamellar structure of the polymer. The contrast covers height variation in the 0–100 nm range in part a, amplitude variation in the 0–0.5 V range in part b, and phase variation in the 0–80° range in part c. (d) A 2D FFT pattern corresponding to the amplitude image (part b).

are indications that lamellae with a certain thickness appear periodically, or in other words, such lamellae are dominant in the view area. The circular average of the power spectrum of the 2D FFT pattern shows the first maximum at  $0.00425 \text{ nm}^{-1}$ . Correspondingly, the average repeat unit of the structure feature is about 235 nm. In consideration of the observation that the average thicknesses of the gaps between lamellae is about 35 nm, which were directly measured from the image, the estimated average thickness of the dominated lamellae is about 200 nm. However, many thinner lamellae, as indicated by the arrow in Figure 2a, are visible, too.

They normally have two tapered heads and are embedded between two thick lamellae. Because the average length of the molecules is about 205 nm and also because the rigid and conjugated P-4BCMU molecules cannot be folded, it is reasonable to believe that the lamellae observed in this study are the extended-chain ones formed by the rigid P-4BCMU molecules. This is a structural feature similar to that attained by TEM from the thin film samples with a thickness of about 50 nm.<sup>6–12</sup> Such a structural feature indicates the occurrence of the chain segregation with respect to chain length distribution through the longitudinal and trans-

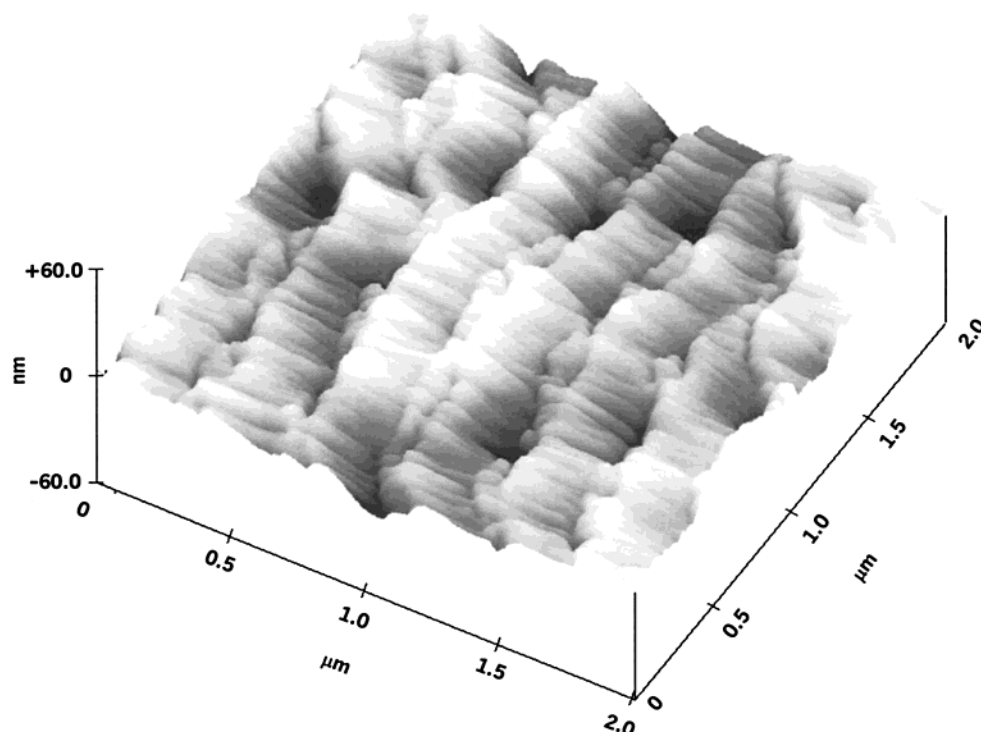


**Figure 4.** 3D AFM height image obtained at higher magnification showing the topographical structure of several lamellae in detail.

versal migration models in lyotropic phase, as suggested in the previous work.<sup>12</sup> Besides the extended-chain lamellae, a fine structure for the lamellae having directors perpendicular to the lamellar directors is also visible but not as clear as reported, possibly due to the smeared effect of the coated gold layer. As mentioned above, SEM images detected by the secondary electron detector mainly provide the topographical variation of a specimen surface, so the results presented here can further reveal some complex topographical structures already self-assembled on the surface of the film samples.

To further gain the physical fundamentals of the topographical structures of the lamellae in more detail, an AFM was applied to investigate the surface profiles of the same sample at different areas. The typical height (a), amplitude (b), and phase (c) images obtained from the same specimen are shown in Figure 3. Figure 3d shows the 2D FFT pattern corresponding to the amplitude image. All three images and the FFT pattern present a lamella-structured feature that is the same as that shown in Figure 2. Obviously, the lamellar feature in the amplitude and phase images is much more visible than that in the height image. Again, the lamellae having an average thickness around 200 nm are in majority and there are some thinner or tapered lamellae embedded between them. (The method used for estimation of the lamellar thickness is the same as that described above.) The fine structure on the lamellae is also visible, in particular in the height image. The AFM observations provide a piece of more clear-cut evidence to demonstrate that some topographical structure had developed on the surface of the film specimens. In the height image, the lamellae are brighter than the areas between them. This indicates that the areas occupied by the lamellae are higher than the areas between them. The height difference indicates valleys or gaps existing between adjacent lamellae. This is physically fundamental to a better understanding of

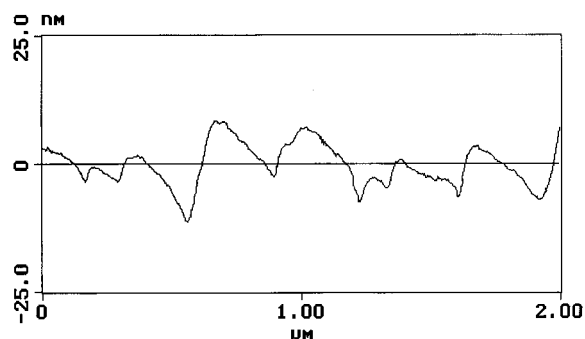


**Figure 5.** One of the surface profiles attained from the cross-section analysis of the height image of Figure 4.

determinability of the structural features with SEM and AFM. The valleys are the imperfections that lead to the clearer amplitude and phase images because the amplitude and phase detecting models show a higher sensitivity to the imperfections.<sup>13</sup>

Now we note that the dominant lamellae shown in the SEM and AFM images have an average thickness of about 200–230 nm and that the number of thin lamellae is very limited. It is hard to believe that the distribution of the lamellar thickness reflects the real distribution of molecular length of this polymer with  $\bar{M}_w/\bar{M}_n = 2.14$ . A part of molecules shorter than 200–230 nm are seemingly “missing” in the view area. To give a clue to this puzzle, it is necessary to further investigate the lamellar structure in 3D space in more detail.

The detailed height variation of individual lamellae was further characterized at a high magnification, as shown in Figure 4 that exhibits a 3D topographical feature of several lamellae in detail. Figure 5 shows one of the surface profiles attained from the cross-section analysis of the height image. Both the 3D image and the surface profile analysis demonstrate a smooth

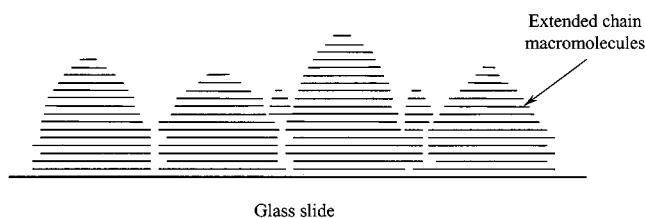


**Figure 6.** Schematic representation showing the cross-sectional feature of extended-chain lamellae on the sample surface. Note the variation in molecular length.

decrease in thickness of the lamellae from the bottom to top. This feature should reflect a gradual decrease in molecular length from bottom to top, as schematically shown in Figure 6. This variation in molecular length with the distance to the surface is an indication why the 2D distribution of lamellar thickness shown in Figures 2 and 3 does not present the real distribution of molecular length. This result further illustrates a special chain segregation occurring along the thickness direction of the film specimen, combining with the 2D chain segregation, as suggested in ref 8. The driving force for such chain segregation also comes from the avoidance or minimization of the defects caused by the chain ends due to the difference in molecular length for individual lamellae. This matter was elucidated in ref 5 in detail.

By the roughness profile analysis in the sampling area in Figure 4, the mean height of the roughness profile is about 4.5 nm, implying that the topographical structure on the surface of this film specimen has an average height of 4.5 nm. In other words, the average depth of the valleys is 4.5 nm for this specimen. Furthermore, we should note that the measured average height 4.5 nm is smaller than the total sample thickness (~500 nm). It is also meaningful to emphasize here that such the topographical morphology was observed in all film samples having different thicknesses varying from 50 nm to 10  $\mu\text{m}$ . However, the average height and the lamellar thickness are a function of the sample thickness and also of the time length when the sample stays in the lyotropic phase. The later effect factor implies a structural evolution gradually occurring in lyotropic phase.

The results presented in this work can help us have a better understanding of the experimental results reported in the former works.<sup>6-12</sup> In the earlier studies,<sup>6-12</sup> TEM was employed to characterize the supramolecular structures of thin film specimens (about 50 nm) of this polydiacetylene. The same extended-chain lamellar structure has been imaged because of the existence of a high electron contrast between the areas occupied by the lamellae and the areas between them. In those studies, the high electron contrast was primarily attributed to a density difference between two areas because the areas between the lamellae consist mainly

of ends of chains having different lengths, and thus its density is lower. It is interesting to note that the topographical structure of the polydiacetylene samples found in this study should provide another piece of evidence to explain the high electron contrast caught by TEM, at least partly. Figure 4 clearly shows the existence of valleys with an average depth smaller than 5 nm between two adjacent lamellae. Naturally, the electron density of lamellae is higher than that of valleys.

## Summary

In summary, the topographical structures of the film samples of the soluble polydiacetylene (P-4BCMU) solidified from its lyotropic liquid crystal phase have been characterized by using SEM and AFM. The observations reveal a structural feature of extended-chain lamellae of the film samples and a 3D chain segregation in a surface layer thinner than 10 nm. The investigation elucidates that in contrast to conventional flexible chain polymers, the topographical structures of such rigid macromolecules are highly dependent on the structures self-assembled already in the lyotropic phase and the solidification will not affect or vary the structure to a great extent.

**Acknowledgment.** We greatly appreciate Professor G. Wegner and Dr. Lieser from the Max-Planck-Institut für Polymerforschung in Germany for providing the polymer. Many thanks are given to Ms. Agness Lim from the Department of Materials, Science of National University of Singapore, for her assistance in using the SEM and to Dr. Lin Yuhui in our institute for his assistance in using the PLM.

## References and Notes

- (1) Flory, P. J. *Proc. R. Soc. London* **1956**, A234, 73.
- (2) Flory, P. J. *Adv. Polym. Sci.* **1984**, 59, 1.
- (3) de Gennes, P. G.; Prost, J. *The Physics of Liquid Crystals*; Clarendon Press: Oxford, England, 1993.
- (4) de Gennes, P. G. *Mol. Cryst. Liq. Cryst. (Lett.)* **1977**, 34, 289.
- (5) Meyer, R. B. In *Polymer Liquid Crystals*; Ciferri, A., Krigbaum, W. R., Meyer, R. B., Eds.; Academia Press: New York, 1988; p 133.
- (6) Albrecht, C.; Lieser, G.; Wegner, G.; *Beitr. Elektronenmikroskop Direktabb. Oberfl. (BEDO)* **1989**, 33, 351.
- (7) Lieser, P. G.; Wang, W.; Albrecht, C.; Schwiegk, S.; Rehahn, M.; Wegner, G. *Polym. Prepr. (Am. Chem. Div. Polym. Chem.)* **1992**, 33, 294.
- (8) Wang, W.; Lieser, G.; Wegner, G. *Liq. Cryst.* **1993**, 15, 1.
- (9) Wang, W.; Lieser, G.; Wegner, G. *Makromol. Chem.* **1993**, 194, 1289.
- (10) Albrecht, C.; Lieser, G.; Wegner, G. *Prog. Colloid Polym. Sci.* **1993**, 92, 111.
- (11) Wang, W.; Hashimoto, T.; Lieser, G.; Wegner, G.; *J. Polym. Sci., Part B Polym. Phys. Ed.* **1994**, 32, 2171.
- (12) Wang, W.; Lieser, G.; Wegner, G. *Macromolecules* **1994**, 27, 1027.
- (13) Magonov, S. N.; Reneker, D. H. *Annu. Rev. Mater. Sci.* **1997**, 27, 175.

MA991596H